Journal Pre-proof

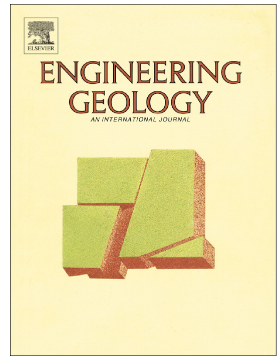

Obtaining suitable logic-tree weights for probabilistic earthquake-induced landslide hazard analyses

M.J. Rodríguez-Peces, J.C. Román-Herrera, J.A. Peláez, J. Delgado, M. Tsige, C. Missori, S. Martino, J. Garrido

PII: S0013-7952(20)30186-1

DOI: https://doi.org/10.1016/j.enggeo.2020.105743

Reference: ENGEO 105743

To appear in: *Engineering Geology*

Received date: 30 January 2020

Revised date: 22 June 2020

Accepted date: 22 June 2020

OBTAINING SUITABLE LOGIC-TREE WEIGHTS FOR PROBABILISTIC EARTHQUAKE-INDUCED LANDSLIDE HAZARD ANALYSES

Rodríguez-Peces, M.J.[a], Román-Herrera, J.C. [a,*]; Peláez, J.A.[b]; Delgado, J.[c]; Tsige, M. [a]; Missori, C.[c]; Martino, S.[d]; Garrido, J.[e]

[a] Department of Geodynamics, Stratigraphy and Paleontology. Faculty of Geological Sciences. University Complutense of Madrid, Madrid, Spain, C/José Antonio Novais, 12, 28040. martinjr@ucm.es, jorom01@ucm.es, meaza@ucm.es

[b] Department of Physics, University of Jaén, Campus Las Lagunillas, Jaén, Spain, 23071. japelaez@ujaen.es

[c] Department of Environment and Earth Sciences, University of Alicante, Alicante, Spain, Ap. Correos 99, 03080. cristina.missori@ua.es, jose.delgado@ua.es

[d] Department of Earth Sciences and Research Center for Geological Risk (CERI), University of Roma "Sapienza", Italy, P.le A.Moro, 5, 00185. salvatore.martino@uniroma1.it

[e] Department of Civil Engineering, University of Granada, Granada, Spain, Campus Fuentenueva, Av. Severo Ochoa s/n, 18071. jega@ugr.es

* Corresponding author: jorom01@ucm.es

Abstract

In this study, an inventory of landslides induced by the 2011 Lorca earthquake (M_w 5.1) has been used in order to develop a new procedure to obtain objective logic-tree weights for a probabilistic earthquake-induced landslide hazard analysis. The 2011 Lorca earthquake triggered more than 250 landslides, mainly of disrupted type. The logic-tree was designed having regard to variability of relevant geotechnical parameters involved in the problem and uncertainties associated with the use of several empirical relationships in order to compute Newmark displacements. For the purpose, the resulting hazard maps were compared with this landslide inventory, and weights estimated for each branch of the logic tree based on these results. The best model for seismic landslide hazard mapping for a moderate earthquake correctly identifies around 72 % of landslide areas. Based on the set of parameters that comprises (depth of failure surface, specific weight, cohesion, friction angle and Newmark displacement model), the corresponding weights were objectively established. These weights are reliable enough for the obtaining seismic landslide hazard maps and may be implemented in similar environments characterized by moderate-low magnitude earthquakes (M_w < 5.5).

Keywords: landslide, earthquake, seismically-induced landslide, hazard map, logic tree.

1. Introduction

The occurrence of earthquake-induced landslides represents a relevant contribution to seismic risk (Bird and Bommer, 2004). Producing hazard maps to delineate areas prone to earthquake-induced landslides is likely the best way to address this issue in our societies. Although several methodologies have been proposed for the production of such maps (Wieczoreck et al., 1985; Luzi et al., 2000; Mulas et al., 2001; Del Gaudio et al., 2003; Jibson, 2011; Rathje and Antonakos, 2011), the method proposed by the United States Geological Survey (Jibson, 1993; Jibson et al., 2000) has been the most widely used in the last two decades. More recently, a new approach, called PARSIFAL (Probabilistic Approach to pRovide Scenarios of earthquake-Induced slope FAilLures), has been proposed (Esposito et al, 2016). This methodology considers different failure mechanisms. It allows comprehensive mapping of earthquake-induced landslide scenarios in terms of exceedance probability of critical threshold values of co-seismic displacements. In the analysis, first-time landslides (due to both rock-slope failures and shallow earth-slides) and reactivations of existing landslides are also considered. PARSIFAL was applied in the framework of seismic microzonation studies in Italy after the 2016-2017 destructive seismic sequence in the Central Apennines (Martino et al., 2019). The methodologies for producing earthquake-induced landslides hazard maps are based on the concept of sliding rigid block (Newmark, 1965) and compute the accumulated displacement of the slope once the earthquake is over (also known as Newmark displacement) through two integrations. Seismic acceleration is integrated to obtain velocity for those portions of the accelerogram record where the acceleration overcomes the yield acceleration (k_y) in slope stability, and then velocity is integrated to obtain displacement. Alternatively, displacements may be computed from empirical relationships that take into account the severity of shaking (earthquake magnitude, peak ground acceleration –PGA–, peak ground velocity –PGV–, Arias intensity –I_A–, etc.) and the yield acceleration in slope stability. The success of this methodology comes from the fact of merging quantitatively the main factors of the problem in a Geographic Information System (GIS) environment: geometry of slopes, geotechnical parameters of slope materials, and severity of seismic ground motion. This allows for the rapid production of hazard maps. This methodology has proved to be very useful for studying the occurrence of small, shallow and disrupted landslides (Jibson et al., 2000; Jibson and Michael, 2009) which is the typology of landslides more frequently induced by earthquakes (Keefer, 1984; Delgado et al., 2011).

The Newmark sliding block methodology has several limitations in relation to the difficulty of incorporating the uncertainties/variability of the three types of variable used in our analysis. As for small sized landslides (such as rock slides and falls), Rodríguez-Peces et al. (2011) showed that the resulting Newmark displacements vary highly depending on the spatial resolution of the digital elevation model (DEM) used to obtain the relief: low resolution DEMs tend to smooth the relief, resulting in high safety factors and yield accelerations, and, moreover, lower Newmark displacements. These authors suggest the use of high resolution DEMs, with pixel size similar to or slightly greater than the size of slope instabilities expected to be induced by earthquakes.

The geotechnical properties of geological materials are another source of limitation. They usually are characterized by inherent variability (Phoon and Kulhawy, 1999). McCrink (2001) and Dreyfus et al. (2013) studied the effect of strength parameters variability on the resulting hazard maps. They compared the resulting maps with the inventories of seismically induced landslides of the 1989 Loma Prieta (M_w = 6.8) and 1994 Northridge (M_w = 6.7) earthquakes, both located in California (USA). Those authors found that maps correctly captured only part of the observed landslides. The proportion of correctly captured ground failures increased when the strength parameters were reduced, but at the cost of excessively increasing the total area of predicted landslides (increasing the size of zones with higher hazard categories). Another related limitation of the present methodology stems from an inability to include spatial variability of strength parameters within the same geological formation (Dreyfus et al., 2013).

Several authors have proposed empirical relationships in order to estimate Newmark displacements (Jibson et al., 2000; Bray and Travasarou, 2007; Jibson, 2007; Saygili and Rathje, 2008; Chousianitis et al., 2016; among others). The use of different relations leads to different displacements. Du et al. (2018) studied the uncertainty associated with the use of different empirical relations. These authors prove that uncertainties are greater for those relations based on a single ground motion parameter (PGA, PGV or I_A) when compared with those that consider multiple ground motion parameters (usually two). Dreyfus et al. (2013) show that the results of a given model depend less on the Newmark displacement relationship and ground motion parameters of the earthquake than on the strength parameters used.

Monte Carlo simulations have been used to manage the variability of variables (Refice and Capolongo, 2002; Murphy and Mankelow, 2004), although the high volume of data required limits use of this approach. Rathje and Saygili (2009) propose the use of the logic-tree methodology instead. This methodology is widely used in seismic hazard studies (Kulkarni et al., 1984; Bommer and Scherbaum, 2008; Delavaud et al., 2012; IGN, 2017; among others). A set of nodes form a logic-tree, with one node for each variable of the problem. From each node, several branches depart representing the discrete values that the corresponding variable can take. Each branch is characterized by its weight that reflects its relative relevance from the analyst's point of view. The sum of the weights corresponding to the branches of each node is always one. The end branches of the logic tree weight are the product of its path branches weights. The result of a logic-tree study is obtained as the weighted summation of the results obtained at the n-branches of the model. Finally, a hazard value is estimated for each path through the logic-tree, with the total weighting of each hazard value being the product of the individual branch weights. Wang and Rathje (2015) used the logic-tree methodology to incorporate the variability in strength parameters of materials in an area.

The main problem when using this logic-tree methodology is how weights are estimated/set for each branch. Several possibilities are found in literature: sometimes they are based on an expert judgement or subjective considerations derived from available information (e.g. IGN, 2017) and sometimes they are set based on probabilistic models (e.g. Wang and Rathje, 2015). At present, there is no proper method to set weights objectively.

In this study, we have worked with the inventory of landslides induced by the 2011 Lorca earthquake with M_w 5.1 that triggered far more slope instabilities than any other instrumental earthquake recorded in Spain (Alfaro et al., 2012; Rodríguez-Peces et al., 2013). We have used the well-known data of this event (magnitude, ground motions, landslides location, and geotechnical parameters) to analyze the efficiency of the seismically-induced landslide hazard maps obtained using a logic tree. This tree was designed in order to consider variability of geotechnical parameters and uncertainties associated with the use of several empirical relationships to compute Newmark displacement. The aim is to compare the resulting hazard maps with the available landslide inventory and propose a new method to estimate objectively weights for each branch based on those results. These weights will form the basis for research in progress with the aim of producing seismic landslide hazard maps for moderate-low magnitude events (M_w < 5.5) along the main lifelines in Southern Spain.

2. The 2011 Lorca earthquake

The Lorca earthquake occurred on May 11, 2011, at 6:47 pm (local time) with a magnitude of M_w 5.1 (IGN, 2011). It had a focal depth of 4 km and it was located at less than 5 km NE of the city of Lorca (Murcia, SE Spain). It was preceded by a M_w 4.5 foreshock at 5:05 pm (local time) and followed by multiple low magnitude (M_w< 4.0) aftershocks. This seismic event caused nine fatalities, and damaged more than 1000 buildings causing economic losses of more than 1200 million euros (following Martínez-Díaz et al., 2012). The event occurred in a segment of the Alhama de Murcia Fault, the main active fault in the area (Fig. 1). This fault accommodates a fraction (around 0.1-0.6 mm/yr) of the approximately 5 mm/yr on the convergence along the Nubian and Eurasian plates boundary (Masana et al., 2004).

The local ground motion caused by this seismic event was recorded by the accelerograph stations of the Spanish strong ground motion network, managed by the Spanish Instituto Geográfico Nacional (IGN). Unfortunately, only one station was located within the epicentral area, where all induced landslides occurred (Fig. 1). Peak ground acceleration (PGA) reached a value of 0.36 g (N-S component) at LOR station (see location in Fig. 1), although PGA varied significantly between horizontal components (Fig. 2a) due to directivity effects (López-Comino et al., 2012). Average PGA values (computed as geometric mean) varied from 0.24 g at LOR station to less than 0.05 g at stations located 20 km (or more) from the epicenter. Average horizontal Arias Intensity (I_A) varied between 0.24 m/s at LOR station and less than 0.02 m/s at distances above 20 km (Fig. 2b).

Newmark displacements have been computed (Fig. 2c) from accelerograms recorded at LOR station following the algorithm described by Jibson (1993). k_y values are fixed (0.01, 0.02, 0.03, 0.04, 0.05, 0.06, 0.08, 0.10, 0.125, 0.15, 0.20, 0.25 and 0.30 g) and thereafter cumulative displacement was computed by integration of those parts of accelerograms where ground acceleration was greater than these yield acceleration values.

The 2011 Lorca earthquake triggered more than 250 landslides (Fig. 1), mainly of disrupted type such as rock/soil falls, soil slides and rock avalanches (Fig. 3). Alfaro et al. (2012) mapped them immediately in the aftermath of the earthquake. As these authors point out, it is not possible to discriminate which event (fore/main shock) triggered these landslides because foreshock and mainshock occurred close in time to each other. Therefore, they were all considered to be triggered by the mainshock. In this regard, all landslides can be considered as first-generation instabilities, and therefore they are not the result of reactivation of prior cases. A common characteristic of all landslides is their small size. Volume was estimated from thickness and the area covered by debris in the deposition area. The resulting volumes show that about 20 % of slope instabilities had very small volumes (<0.1 m^3) and only 50 % of them had volumes above 1 m^3 (Fig. 4). Although these sizes appear to be relatively small, many of them caused a lot of damage and cuts on roads and infrastructures, as well as significant social concern.

Most of inventoried landslides were developed in steep slopes involving mainly four lithological groups (Fig. 1): 1) Calcareous sandstones and limestones; 2) conglomerates, sandstones and argillites; 3) marls and gypsums; and 4) phyllites and quartzites (Rodríguez-Peces et al., 2013). In addition, the Lorca earthquake took place close to the start of the dry summer season, and those lithological groups were in dry conditions (no soil/rock saturation).

The distribution of slope instabilities related to the 2011 Lorca earthquake was compared with prior earthquake-triggered landslide hazard maps (Rodríguez-Peces et al., 2013): a probabilistic map considering the occurrence of the most probable earthquake for a 475-year return period in the Lorca Basin (M_w 5.0), and a deterministic map with the occurrence of a M_w 5.1 earthquake equivalent of the 2011 Lorca event. In both cases, these authors found that the most frequent values of Newmark displacement related to the slope instabilities triggered by such moderate earthquakes were lower than 2 cm. These results concur with the critical displacement value of 2 cm proposed by Wilson and Keefer (1985) for disrupted rock falls similar to the case in Lorca.

3. Methodology

3.1. Logic-tree approach

A logic-tree approach is proposed in order to incorporate the epistemic uncertainties in the procedure for computation of earthquake-induced landslide maps, for each source of uncertainty. The structure of the logic tree was divided into three parts having regard to the uncertainties related to the slope instability size (i.e., depth of the failure surface), geotechnical parameters (i.e., specific weight, cohesion and friction angle) and Newmark displacement regression models (Fig. 5).

In the first section of this logic tree, the variability of the depth of the failure surface was taken from the frequency histogram of the sliding block size according to the slope instability inventory of the 2011 Lorca earthquake (Fig. 6). The branches of the logic tree were defined by the values of the depth of the failure surface (t) of 0.5, 1.0, 2.0 and 3.0 m.

For the second section of the logic tree, different values of specific weight, cohesion and friction angle were assigned to each lithological unit (Tables 1 and 2). These strength parameters were derived from data from 163 geotechnical boreholes and 20 direct shear tests (68 values of specific weight, 40 values of cohesion and friction angle), as well as 114 geomechanical field surveys and 14 in situ testings (544 values of cohesion and friction angle) performed in the Lorca area (Fig. 1) on outcropping rock masses and soil deposits. Previous studies on seismically induced landslides concluded that instabilities developed in rocky materials are controlled by pre-existing fractures (Keefer, 1984). For this reason, cohesion and friction angle values for rock-type lithological groups mostly correspond to rock-mass joints. Then, the strength parameters of joints in rock-type materials were estimated using Barton-Bandis failure criterion (Barton and Choubey, 1977) regarding the thickness of the fallen rock-blocks. Nevertheless, this failure can occur through the intact material as well as pre-existing discontinuities in relatively homogeneous materials, such as soils.

In order to include the variability of shear strength parameters in the logic-tree procedure, Wang and Rathje (2015) used the three-point estimation of the normal distribution that retains the mean and standard deviation of the data distribution (Keefer and Bodily, 1983). However, these authors assumed different values of coefficients of variation (mean divided by standard deviation) due to the lack of enough data for a suitable statistical analysis. In this work, as stated above, we have a large amount of data that has been statistically processed using the IBM SPPS Statistic 25 statistical software (IBM Corp., 2017). Thereafter, the most likely, low and high values of each geotechnical parameter have been taken as 50, 10, and 90 percentiles (Tables 1 and 2) representing respectively μ and μ ± 1.33σ. These values represent the logic tree branches for this section.

As for the third section of the logic tree we have selected 10 Newmark displacement empirical models from the large number of available relationships (Table 3). Here the only models that apply to the case were used taking into account the available data on the 2011 Lorca earthquake. Specifically, we only selected those relationships including PGA or I_A as independent variables. The use of this large amount of Newmark displacement regression models can be seen as an attempt to incorporate the widest possible range of displacement values and epistemic uncertainties. This is especially relevant in the study area, since no local displacement model is currently available.

Finally, a new software code was developed in order to obtain the landslide hazard maps in terms of Newmark displacement considering the different branches of the logic tree (Román-Herrera et al., 2018). That semi-automatic code was written in Python using a geographic information system (ArcGIS© 10 software). The code only considers areas with slope above 10° for computing Newmark displacements.

3.2. Procedure for obtaining weights on logic tree branches

A large number of earthquake-induced landslide hazard maps in terms of the Newmark displacement were obtained taking into account the variability of all variables included in the logic tree. Selecting the best parameter set and model for seismic landslide hazard mapping was performed by comparing the locations of predicted landslides for all models with the inventory of landslides triggered by the 2011 Lorca earthquake.

The prediction efficiency of each combination of parameter sets and empirical models was evaluated based on the success rate percentage of the estimated hazard map by combining the efficiency parameters used by McCrink (2001). Applying his procedure, a higher level of efficiency should be found maximizing the percentage of correctly identified landslide (%GFC = % Ground Failure Capture) and minimizing the percentage of the total area identified as landslides (%TAC = % Total Area Covered). Considering that landslides triggered by the 2011 Lorca earthquake have been related to Newmark displacements lower than 2 cm (Rodríguez-Peces et al., 2013), failures located over areas with Newmark displacement higher than 1 cm were considered for computing the %GFC, while %TAC was estimated considering the area with Newmark displacement higher than 1 cm over the total studied area. This threshold value of Newmark displacement is related to a moderate seismic hazard category with a probability of landslide higher than 2 % (Jibson and Michael, 2009).

Taking into account both parameters, another efficiency criterion can also be established by maximizing the difference between %GFC and %TAC (%Difference =%GFC - %TAC), which penalizes hazard maps that have a high %GFC value simply because they predict a very large area with landslides (%TAC). Finally, the success rate percentage (%SR) of the various hazard maps was estimated by multiplying %GFC and %Difference, and, therefore, maps can be ordered from the highest to the lowest success rate.

The weights on logic tree branches (low, most likely and high) have been obtained taking into account the success rate (%SR) corresponding to the variability of each variable, fixing the value of the remaining variables. Following this procedure, the weight of each branch is estimated from 0 to 1 in proportion to the success rates obtained for each variable. The branch with the highest %SR is assigned the greatest weight; the next branch with a smaller %SR has a lower weight, and so on. The sum of the branches weights corresponding to the same node must be equal to one.

The final weights associated with each landslide hazard map have been calculated by multiplying the partial weights obtained previously for each branch from the first section of the logic tree (i.e., depth of the failure surface) going through the second part (i.e., specific weight, cohesion and friction angle) to the last part (i.e., Newmark displacement regression models).

The variability of results depending on the different values for the considered variables (landslide size, geotechnical parameters, Newmark displacement regression model) was analyzed using the SPPS© statistical software (IBM Corp., 2017).

4. Results and Discussion

Having applied the above-described methodology, 1080 landslide hazard maps in terms of Newmark displacement were obtained regarding the 2011 Lorca earthquake (M_w 5.1) and the variability of all variables through the logic tree. This event occurred under dry conditions of slopes. Figure 7 shows the models using the efficiency parameters as described by McCrink (2001). In general, the percentage of correctly identified landslide areas (%GFC) is between 24 and 86 %, while the difference between the percentage of correctly identified landslide areas (%GFC) and the percentage of total area identified as landslides (%TAC) is between 4 and 55 %.

The highest percentage of success rate (%SR) of any seismic landslide hazard map regarding the Lorca earthquake is 38.5 % (optimum model in Fig. 7), which corresponds to 15.1 % of the total area identified as landslides (%TAC) and 70.0 % of correctly identified landslide areas (%GFC). In addition, %Difference = 54.9 % is also the highest value. These values are higher, especially the %Difference, than those found by McCrick (2001) with values lower than 38 %. Therefore, this hazard map comprises the following set of parameters:

- Depth of the failure surface (t): 3.0 m.
- Specific weight (ϒ): percentile 10.
- Cohesion (c): percentile 10.
- Friction angle (Φ): percentile 90.
- Newmark displacement model: RS09 by Rathje and Saygili (2009).

Previous set of parameters represents the optimum case (Figures 7 and 8a). This map shows areas with very high seismic landslide hazard (Newmark displacements greater than 15 cm) favoring a large number of correctly predicted slope instabilities (Fig. 8a). On the other hand, the map with the highest percentage of landslide areas correctly identified (%GFC = 85.6 %) corresponds with a very high total area identified as landslides (%TAC = 74.3 %) and very low %Difference = 9.7 % (Figure 8b). These results are related to the weakest geotechnical conditions with regard to slope stability. Newmark displacements greater than 10 cm should have corresponded to the triggering of much larger landslides than was actually the case. These high Newmark displacements are also a function of the extreme values of the input set of parameters. In this regard, this map significantly overpredicts what actually happened, being an unrealistic characterization of conditions during the earthquake.

4.1. Influence of variability of slope instability size

The variation in success rate (%SR) has been analyzed taking into account the depth of the failure surface (Fig. 9a).The maximum %SR values are quite similar, regardless of depth as the computed percentages closely range from 36.4 to 38.5 %, varying from 0.5 up to 3.0 m depth. However, considering the median and mean values, the %SRs of the models improve as the depth of the failure surface increases. In particular, the median %SRs obtained for depths of 0.5 and 1.0 m are almost the same (10.6 and 10.7 % respectively), while %SRs increase for depths of 2.0 and 3.0 m (19.0 and 21.5 % respectively). Similar patterns are observed for mean values: 14.0 % for depths of both 0.5 and 1.0 m, and 18.3 and 22.5 % for depths of 2.0 and 3.0 m, respectively. These results are consistent with a usual geotechnical behavior in relation to slope stability. As the depth of failure surface (i.e., size) of landslides increases, the effect of cohesion decreases. Therefore, if all other parameters remain constant, increasing the depth will decrease the shear resistance and increase landslide susceptibility.

From a statistical point of view (t and Mann-Whitney tests), there are no significant differences between means and medians of the SR samples of 0.5 and 1.0 m. Thus, they could be considered together in a single branch of the logic tree instead of two. Consequently, the node related to the variability of slope instability size could have three branches (1.0, 2.0 and 3.0 m), rather than the four initially considered.

4.2. Influence of variability of geotechnical parameters

The variation in success rate (%SR) has also been analyzed considering the specific weight variability (Fig. 9b). The maximum %SR values are the same regardless of the specific weight: 38.5 % for percentiles 10, 50 and 90, respectively. Moreover, the improvement in %SRs is very small, with a very slight increase as regards the percentile. In particular, the median %SRs are 13.2, 14.4 and 16.6 % for percentiles 10, 50 and 90, respectively. A similar pattern is observed for mean values: 16.8, 17.1 and 17.8 % for percentiles 10, 50 and 90, respectively. From a statistical point of view (t and Mann-Whitney tests), there are no significant differences between mean and median values concerning %SR samples for percentiles 10, 50 and 90. Therefore, the %SR is not affected by the variability of the specific weight and a fixed value should be used to perform the calculations needed to obtain the %SR (e.g., percentile 90). In this regard, there is no need to use the specific weight as a node in the logic-tree procedure as initially planned.

Considering the variation in %SR with respect to cohesion variability (Fig. 9c), the maximum %SR values are very different and they decrease as the percentile increases: 38.5, 34.3 and 20.9 % for percentiles 10, 50 and 90, respectively. In addition, the median %SRs are 27.1, 12.0 and 9.7 % for percentiles 10, 50 and 90, respectively. A similar pattern is observed concerning mean values: 26.2, 15.6 and 9.8 % for percentiles 10, 50 and 90, respectively. These results concur with usual geotechnical behavior, as increasing the cohesion will increase the shear resistance and decrease landslide susceptibility. From a statistical point of view (t and Mann-Whitney tests), there are significant differences between means and medians regarding %SR samples of percentiles 10, 50 and 90. Therefore, the %SR is affected by the variability of the cohesion and should be used as a node with three branches in the logic-tree procedure.

Finally, the variation in %SR with respect to the friction angle variability is shown in Figure 9d. The maximum %SR values are quite different and they decrease as the percentile increases: 28.0, 34.1 and 38.5 % for percentiles 10, 50 and 90, respectively. In addition, the median %SRs are 12.4, 19.4 and 15.2 % for percentiles 10, 50 and 90, respectively. Similar patterns are observed concerning mean values: 12.9, 19.5 and 19.3 % for percentiles 10, 50 and 90, respectively. These results also agree with a typical geotechnical behavior, as decreasing the friction angle will decrease the shear resistance and increase landslide susceptibility. From a statistical point of view (t and Mann-Whitney tests), there are significant differences between mean and median values regarding %SR samples for percentiles 10, 50 and 90. Therefore, the %SR is affected by the variability of the friction angle and should be used as a node with three branches in the logic-tree procedure.

4.3. Influence of variability of Newmark displacement regression models

The variation in success rate (%SR) has been analyzed (Fig. 9e) taking into account Newmark displacement regression equations. The maximum %SR values are similar regardless of the equation, ranging from 32.9 to 38.5 % (Table 4). Model RS09 by Rathje and Saygili (2009) is the best model with the highest %SR value (38.5 %). The same pattern was found taking into account the median and mean values (Table 4). From a statistical point of view (Fisher, Kruskal-Wallis and Mood tests), there are no significant differences between means and medians regarding %SR samples for J07_1 and J07_2 models, so they could be considered to be a single node of the logic tree rather than two. In addition, there are no significant differences between means and medians values for the remaining equations (J07_3, J07_4, BT07, SR08_1, SR08_2, RS09, HL11 and JL18 models). Therefore, they coud be simplified as a single node of the logic tree instead of eight, applying one of the models with the highest %SR (e.g., RS09 model) to obtain the best results. Therefore, the %SR is affected by the variability of the

Newmark displacement regression model and should be used as a node with two branches in the logic-tree procedure.

4.4. Weights of the variables and hazard maps

In the first part of the logic tree, the distribution of weights in each branch related to the depth of the failure surface was taken from the frequency histogram of the sliding block size (Fig. 6). As indicated in the previous section, the branches of the logic tree should be simplified by depths of 1.0, 2.0 and 3.0 m. For each one, the assigned weights are 0.528, 0.405 and 0.067, respectively.

In the second part of the logic tree, although it has been pointed out that there is no need to use the specific weight as a node, we have obtained the weights for this variable anyway (Fig. 10a). The mean values are very similar: 0.323, 0.330 and 0.347 for percentiles 10, 50 and 90, respectively. Equivalent weights are obtained if median values are considered 0.333 for percentiles 10, 50 and 90. These results show that the three branches corresponding to percentiles 10, 50 and 90 have the same weight (i.e., 0.333), reinforcing our proposal of remove them from the logic tree and therefore using a fixed value of the specific weight.

Considering the variable cohesion, mean values of the weights are quite different and decrease as the percentile increases: 0.533, 0.281 and 0.186 for percentiles 10, 50 and 90, respectively (Fig. 10c). Similar weights are obtained if median values are considered: 0.587, 0.227 and 0.186 for percentiles 10, 50 and 90, respectively.

As a final point on this part of the logic tree, the friction angle variable shows mean values of the weights that are slightly different: 0.269, 0.384 and 0.347 for percentiles 10, 50 and 90, respectively (Fig. 10b). Considering the median values, we obtain very similar weights: 0.250, 0.390 and 0.360 for percentiles 10, 50 and 90, respectively.

As for the last part of the logic tree, mean and median weights obtained by Newmark displacement regression models are also very similar for each particular model (Table 5). Although individual weights may seem very similar (Fig. 10d), the median values are significantly different from each other from a statistical standpoint (Kruskal-Wallis and Mood tests). This fact means that all of them should be taken into account and cannot be simplified, as suggested above. However, there are no significant differences (Fisher test) between mean weights for HL11 and JL18 models, so they could be considered to be a single node of the logic tree instead of two, applying the highest %SR model (i.e., HL11 model) to obtain the best results. In addition, there are no significant differences between mean values for J07_3, J07_4, SR08_2 and RS09 relationships. Thus, they could be simplified as a single node of the logic tree instead of four, applying one of the models with the highest %SR (i.e., RS09 model) to obtain the best results. Therefore, the %SR is affected by the variability of the Newmark displacement regression model and should be used as a node with at least six branches in the logic-tree procedure. These branches comprise the J07_1, J07_2, BT07, SR08_1, RS09 and HL11 models, with weights of 0.120, 0.144, 0.170, 0.179, 0.200 and 0.188, respectively. The highest weight is 0.200, corresponding with model RS09 by Rathje and Saygili (2009) which, as stated above, is the model with the highest %SR value.

The weights objectively obtained here for each branch of the logic tree are quite different from those used by Wang and Rathje (2015). Due to the lack of sufficient input data of the various variables, these authors assumed the three-point estimation of the normal distribution proposed by Keefer and Bodily (1983), in which weights are fixed statistically: 0.3, 0.4 and 0.3 for the maximum (percentile90), best (percentile50) and minimum (percentile10), respectively. In addition, Wang and Rathje (2015) subjectively modified these weights to give more or less relevance to some of the branches.

Taking into account all partial weights for each branch in the logic tree, the final weight for each resulting hazard map was obtained. Having regard to the set of parameters that comprises the above-mentioned landslide hazard map with the highest success rate (Fig. 8a), the total weight of that map is 0.00062. However, the highest total weight is 0.00394, which corresponds to a landslide hazard map (Fig. 8c) characterized by the following combination of factors: 2.0 m depth of failure surface , percentile 10 of specific weight, percentile 10 of cohesion, percentile 90 of friction angle, and Newmark displacement model SR08_1 by Saygili and Rathje (2008). The success rate percentage (%SR) of that map with regard to the Lorca earthquake is 38.3 %, which corresponds to 19.5 % of the total area identified as landslides (%TAC) and 72.4 % of correctly identified landslide areas (%GFC). Moreover, %Difference = 52.9 % is also high. These results are quite similar to those obtained with the combination of factors with the highest success rate (Fig. 7), but having a slightly higher weight. We suggest the combination of factors with the highest weight as the best in order to obtain the probabilistic hazard map.

In a previous study, hazard maps were obtained using deterministic procedures (Rodríguez-Peces et al., 2013); all variables were set to their average value and their variability was not taken into account. In that study, the %SR was extremely low (0.1 %) with a %TAC of 0.1 % and 2.7 % of correctly identified landslide areas (%GFC). In addition, %Difference = 2.7 % is also very low. These data indicate that better results are obtained performing a probabilistic analysis rather than applying a deterministic one.

5. Conclusions

This research shows that objective weights have been estimated for each branch of a logic-tree procedure applied to a probabilistic earthquake-induced landslide hazard analysis, and more specifically to a moderate seismic event, such as the 2011 Lorca earthquake in Spain. Moreover, the methodology used is proposed for the first time, making it possible to discard variables in the logic-tree procedure and quantify objective weights, unlike the usual way of performing this procedure (i.e., subjective weights). Therefore, the proposed method makes it possible to discard expert judgement as a method of assigning weights in the logic-tree procedure and to use objective criteria instead, if the required input data are available. The case studied here has the advantage of involving failures of a similar type (falls and shallow disrupted slides) that affected a reduced set of lithologies. This allowed us to assume a simplified mechanism of slope failure for computing critical acceleration and Newmark displacement values.

The best model in order to produce seismic landslide hazard mapping for a moderate earthquake have an excellent success rate and about 72 % of correctly identified landslide areas (Fig. 7). This model comprises the following set of parameters: depth of failure surface of 2 m, percentile 10 of specific weight, percentile 10 of cohesion, percentile 90 of friction angle, and Newmark displacement model SR08_1 by Saygili and Rathje (2008).

Considering the influence of the variability of slope instability size, we have concluded that the node of the logic tree should have three branches (1.0, 2.0 and 3.0 m). Regarding the influence of the variability of geotechnical parameters, we found that it is not necessary to use the specific weight as a node in the logic-tree procedure and instead a fixed value of specific weight should be used. However, cohesion, friction angle and Newmark displacement models are relevant variables for consideration as nodes of the logic tree.

All weights objectively obtained here will represent the basis for a research in progress with the aim of producing earthquake-induced landslide hazard maps for moderate-low magnitude events (M_w < 5.5) along the main lifelines in Southern Spain, where the dry condition of slopes considered here are common. In addition, the proposed methodology may be implemented in other regions to obtain weights for each branch of the logic tree for seismically-induced landslide hazard studies.

Acknowledgements

This study was partially funded by research projects CGL2015-65602-R (MINECO/FEDER, UE), CGL2017-83931-C3-1-P (MINECO), the Programa Operativo FEDER Andalucía 2014-2020 – call made by the University of Jaen 2018, and research groups “Planetary Geodynamics, Active Tectonics and Related Risks”, UCM-910368 of the University Complutense of Madrid, and “Applied Geology and Hydrogeology” VIGROB-184 of the University of Alicante. The authors are very grateful to the editor, Dr. Janusz Wasowski, and the two anonymous reviewers whose comments helped to improve this paper.

References

Alfaro, P., Delgado, J., García-Tortosa, F.J., Lenti, L., López, J.A., López-Casado, C., Martino, S., 2012. Widespread landslides induced by the Mw 5.1 earthquake of 11 May 2011 in Lorca. SE Spain. Eng. Geol. 137-138, 40-52.

Ambraseys, N., Douglas, J.R., Sarma, S.K., & Smit, P.M., 2005. Equations for the Estimation of Strong Ground Motions from Shallow Crustal Earthquakes Using Data from Europe and the

Middle East: Horizontal Peak Ground Acceleration and Spectral Acceleration. B. Earthq. Eng. 3, 1-53.

Barton, N., Choubey, V., 1977. The Shear Strength of Rock Joints in Theory and Practice. Rock Mechanics 10(1-2), 1-54.

Bird, J.F., Bommer, J.J., 2004. Earthquake losses due to ground failure. Eng. Geol. 75, 147-179.

Bray, J.D., Travasarou, T., 2007. Simplified procedure for estimating earthquake-induced deviatoric slope displacements. J. Geotech. Geoenviron. 133, 381-392.

Bommer, J.J., Scherbaum, F., 2008. The Use and Misuse of Logic Trees in Probabilistic Seismic Hazard Analysis. Earthq. Spectra 24(4), 997-1009.

Chousianitis, K., Del Gaudio, V., Sabatakakis, N., Kavoura, K., Drakatos, G., Bathrellos, G.D., Skilodimou, H.D., 2016. Assessment of earthquake-induced landslide hazard in Greece: from arias intensity to spatial distribution of slope resistance demand. Bull. Seismol. Soc. Am. 106 (1), 174-188.

Del Gaudio, V., Pierri, P., Wasowski, J., 2003. An approach to time-probabilistic evaluation of seismically induced landslide hazard. Bull. Seismol. Soc. Am. 93(2), 557–569.

Delavaud, E., Cotton, F., Akkar, S., Scherbaum, F., Danciu, L., Beauval, C., Drouet, S., Douglas, J., Basili, R., Sandikkaya, A., Segou, M., Faccioli, E., Theodoulidis, N., 2012. Toward a ground-motion logic tree for probabilistic seismic hazard assessment in Europe. J. Seismol. 16(3), 451-473.

Delgado, J., Peláez, J.A., Tomás, R., García-Tortosa, F.J., Alfaro, P., López Casado, C., 2011. Seismically-induced landslides in the Betic Cordillera (S Spain). Soil Dyn. Earthq. Eng. 31, 1203-1211.

Dreyfus, D., Rathje, E.M., Jibson, R.W., 2013. The influence of different simplified sliding block models and input parameters on regional predictions of seismic landslides triggered by the Northridge earthquake. Eng. Geol. 163, 41-54.

Du, W., Huang, D., Wang, G., 2018. Quantification of model uncertainty and variability in Newmark displacement analysis. Soil Dyn. Earthq. Eng. 109, 286-298.

Esposito, C., Martino, S., Pallone, F., Martini, G., Romeo, R., 2016. A methodology for a comprehensive assessment of earthquake-induced landslide hazard, with an application to pilot sites in Central Italy. In: Landslides and engineered slopes. Experience, theory and practice, Taylor and Francis Inc. 2, 869-877.

García-Mayordomo, J., Insua-Arévalo, J.M., Martínez-Díaz, J.J., Jiménez-Díaz, A., Martín-Banda, R., Martín-Alfageme, S., Álvarez-Gómez, J.A., Rodríguez-Peces, M., Pérez-López, R., Rodríguez-Pascua, M.A., Masana, E., Perea, H., Martín-González, F., Giner-Robles, J., Nemser, E.S., Cabral, J. and the QAFI Compilers Working Group, 2012. The Quaternary Faults Database of Iberia (QAFI v.2.0). J. Iber. Geol. 38, 285-302.

Hsieh, S.Y., Lee, C.T., 2011. Empirical estimation of Newmark displacement from the Arias intensity and critical acceleration. Eng. Geol. 122, 34-42.

IBM Corp. (2017). IBM SPSS Statistics for Windows, Version 25.0. Armonk, NY: IBM Corp.

IGN (Instituto Geográfico Nacional), 2011. Informe del sismo de Lorca del 11 de mayo de 2011. Instituto Geográfico Nacional. 132 pp. Available at the web site http://www.ign.es

IGN (Instituto Geográfico Nacional), 2017. Actualización de mapas de peligrosidad sísmica de España 2012. Gobierno de España. Ministerio de Fomento. Madrid. 267 p.

Jia-Liang, J., Yin, W., Dan, G., Ren-Mao, Y., Xiao-Yan, Y., 2018. New Evaluation Models of Newmark Displacement for Southwest China. Bull. Seismol. Soc. Am. 108(4), 2221-2236.

Jibson, R.W., 1993. Predicting earthquake-induced landslide displacements using Newmark's sliding analysis. Transportation Research Record, 1411, 9-17.

Jibson, R.W., Harp, E.L., Michael, J.A., 2000. A method for producing digital probabilistic seismic landslide hazard maps. Eng. Geol. 58, 271-289.

Jibson, R.W., 2007. Regression models for estimating coseismic landslide displacement. Eng. Geol. 91, 209-218.

Jibson, R.W., 2011. Methods for assessing the stability of slopes during earthquakes—A retrospective. Eng. Geol. 122(1-2), 43-50.

Jibson, R.W., Michael, J. A., 2009. *Maps showing seismic landslide hazards in Anchorage, Alaska*. U.S. Geological Survey Scientific Investigations Map 3077, scale 1:25,000, 11 pp.

Keefer, D.K., 1984. Landslides caused by earthquakes. Geol. Soc. Am. Bull. 95, 406-421.

Keefer, D.L., Bodily, S.E., 1983. Three point approximations for continuous random variables. Manag. Sci. 595-609.

Kulkarni, R.B., Youngs, R.R., Coppersmith, K.J., 1984. Assessment of Confidence Intervals for results of Seismic Hazard Analysis. Proc. 8th World Conference on Earthquake Engineering. San Francisco. California. Vol. I. 263-270.

López-Comino, J.A., Mancilla, F.L., Morales, J., Stich, D., 2012. Rupture directivity of the 2011 Mw 5.2 Lorca earthquake (Spain). Geophys. Res. Lett. 39, L03301.

Luzi, L., Pergalani, F., Terlien, M.T.J., 2000. Slope vulnerability to earthquakes at subregional scale, using probabilistic techniques and geographic information systems. Eng. Geol. 58, 313-336.

Martínez-Díaz, J.J., Béjar-Pizarro, M., Álvarez-Gómez, J., Mancilla, F., Stich, D., Herrera, G., Morales, J., 2012. Tectonic and seismic implications of an intersegment rupture. The damaging May 11th 2011 M_w 5.2 Lorca, Spain, earthquake. Tectonophysics 547, 28-37.

Martino, S., Battaglia, S., D’Alessandro, F., Della Seta, M., Esposito, C., Martini, G., Pallone, F., Troiani, F. (2019). Earthquake-induced landslide scenarios for seismic microzonation: application to the Accumoli area (Rieti, Italy). B. Earthq. Eng. doi:10.1007/s10518-019-00589-1.

Masana, E., Martínez-Díaz, J.J., Hernández-Enrile, J.L., Santanach, P., 2004. The Alhama de Murcia fault (SE Spain), a seismogenic fault in a diffuse plate boundary: Seismotectonic implications for the Ibero-Magrebian region. J. Geophys. Res. 109(1), 17 pp.

McCrink, T.P., 2001. Regional earthquake-induced landslide mapping using Newmark displacement criteria. Santa Cruz County. California. In: Ferriz, H., Anderson, R. (Eds.). Engineering Geology Practice in Northern California: California Division of Mines and Geology Bulletin 210/Association of Engineering Geologists Special Publication 12, 77-92.

Mulas, J., Ponce de León, D., Martínez, M., Pardo, J.M., 2001. Diseño de una metodología para la zonificación de la inestabilidad de laderas naturales producidas por terremotos. Aplicación a una zona del Pirineo Central (Huesca). V Simposio Nacional sobre Taludes y Laderas Inestables. Vol. III, 1241-1252.

Murphy, W., Mankelow, J.H., 2004. Obtaining probabilistic estimates of displacements on a landslide during future earthquakes. J. Earthq. Eng. 8, 133-157.

Newmark, N.M., 1965. Effects of earthquakes on dams and embankments. Géotechnique 15, 139-160.

Phoon, K., Kulhawy, F.H., 1999. Characterization of geotechnical variability. Can. Geotech. J. 36, 612-624.

Rathje, E.M., Saygili, G., 2009. Probabilistic assessment of earthquake-induced sliding displacements of natural slopes. Bull. N.Z. Natl. Soc. Earthqu. Eng. 42, 18-27.

Rathje, E.M., Antonakos, G., 2011. A unified model for predicting earthquake-induced sliding displacements of rigid and flexible slopes. Eng. Geol. 122(1-2), 51-60.

Refice, A., Capolongo, D., 2002. Probabilistic modeling of uncertainties in earthquake induced landslide hazard assessment. Comput. Geosci. 28, 735-749.

Rodríguez-Peces, M.J., Pérez-García, J.L., García-Mayordomo, J., Azañón, J.M., Insua-Arévalo, J.M., Delgado, J., 2011. Applicability of Newmark method at regional. sub-regional and site scales: seismically induced Bullas and La Paca rock-slide cases (Murcia. SE Spain). Natural Hazards 59, 1109-1124.

Rodríguez-Peces, M.J., García-Mayordomo, J., Martínez-Díaz J.J, 2013. Slope instabilities triggered by the 11th May 2011 Lorca earthquake (Murcia. Spain): comparison to previous hazard assessments and proposition of a new hazard map and probability of failure equation. B. Earthq. Eng. 12, 1961-1976.

Román-Herrera, J.C., Rodríguez-Peces, M.J., Delgado, J., Tsige, M., 2018. GIS tool for semi-automatic hazard assessment of earthquake-triggered landslides. Geological Society of America Abstracts with Programs, 50, 6, Paper 244-1. doi: 10.1130/abs/2018AM-321245.

Sabetta, F., Pugliese, A., 1996. Estimation of response spectra and simulation of nonstationary earthquake ground motions. Bull. Seismol. Soc. Am. 86(2), 337-352.

Saygili, G., Rathje, E.M., 2008. Empirical predictive models for earthquake-induced sliding displacements of slopes. J. Geotech. Geoenviron. 134, 790-803.

Wang, Y., Rathje, E.M., 2015. Probabilistic seismic landslide hazard maps including epistemic uncertainties. Eng. Geol. 196, 313-324.

Wieczorek, G.F., Wilson, R.C., Harp, E.L., 1985. Map showing slope stability during earthquakes in San Mateo County California. U.S. Geological Survey Miscellaneous Investigations Map, I-1257-E. Scale 1:62500.

Wilson, R.C., Keefer, D.K., 1985. Predicting areal limits of earthquake-induced landsliding, in Ziony, J.I., (ed.), Evaluating Earthquake hazards in the Los Angeles Region—An Earth-Science Perspective: U.S. Geological Survey Professional Paper 1360, 317-346.

Author statement

M.J. Rodríguez-Peces: Conceptualization, Methodology, Software, Formal analysis, Writing - Original Draft, Writing - Review & Editing.

J.C. Román-Herrera: Conceptualization, Methodology, Software, Formal analysis, Writing - Original Draft, Writing - Review & Editing.

J.A. Peláez: Formal analysis, Writing - Review & Editing.

J. Delgado: Conceptualization, Methodology, Software, Formal analysis, Writing - Review & Editing.

M. Tsige: Formal analysis, Validation, Writing - Review & Editing.

C. Missori: Investigation, Formal analysis, Writing - Review & Editing.

S. Martino: Investigation, Formal analysis, Validation, Writing - Review & Editing.

J. Garrido: Formal analysis, Writing - Review & Editing.

Declaration of interests

☒ The authors declare that they have no known competing financial interests or personal relationships that could have appeared to influence the work reported in this paper.

☐The authors declare the following financial interests/personal relationships which may be considered as potential competing interests:

Figures

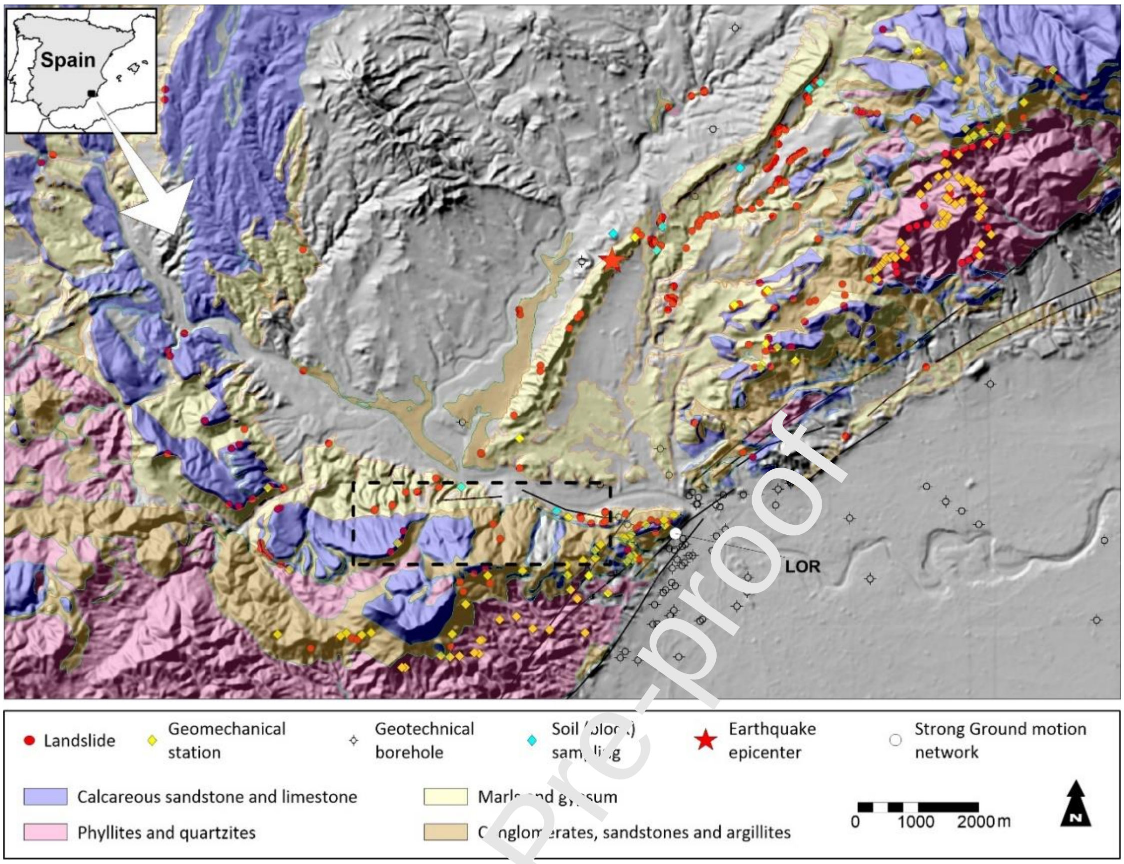

Figure 1. Location map of the study area showing only the lithological groups that were affected by landslides during the 2011 Lorca earthquake (red dots) and location of the in situ testing performed. Continuous black lines: surface traces of main active faults (Alhama de Murcia Fault, cf. García-Mayordomo et al., 2012). Dashed line: perimeter of the area shown in figure 8.

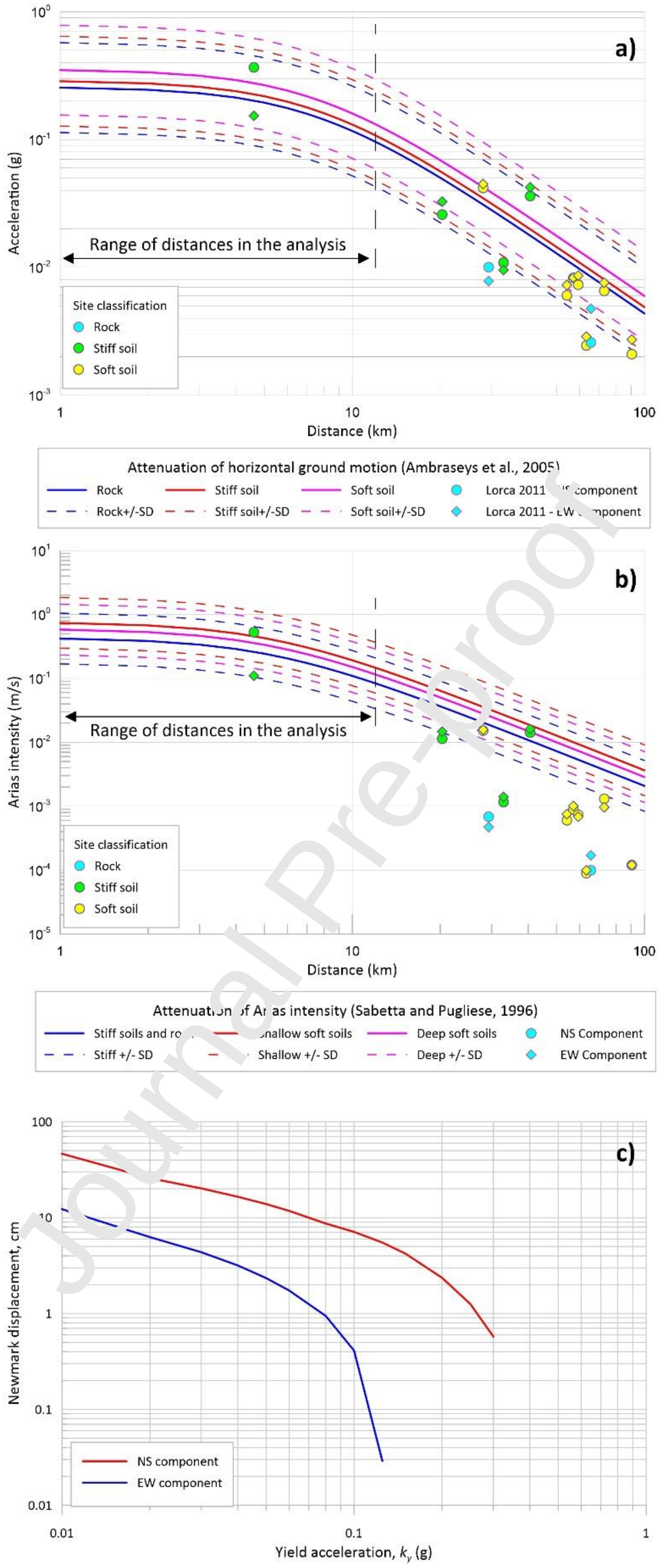

Figure 2. A) Variation of peak ground acceleration (PGA) with epicentral distance for the 2011 Lorca earthquake. Blue line: Ground motion prediction attenuation (GMPA) according to Ambraseys et al. (2005) for rock sites; Red line: same for hard soil sites; Magenta line: same for soft soil sites. B) Variation of Arias intensity (I_A) with epicentral distance according to Sabetta and Pugliese (1996). Blue line: for rock and hard soils sites; Red line: for shallow soft soil sites; Magenta line: for deep soft soil sites. C)

Newmark displacement (D_N) computed for the two horizontal components of ground motion recorded at LOR (Lorca) station. Red line: N-S component; Blue line: E-W component.

Figure 3. Some examples of landslides triggered by the 2011 Lorca earthquake, mainly disrupted ones, such as soil slides (top photos) and rock falls (intermediate and bottom photos).

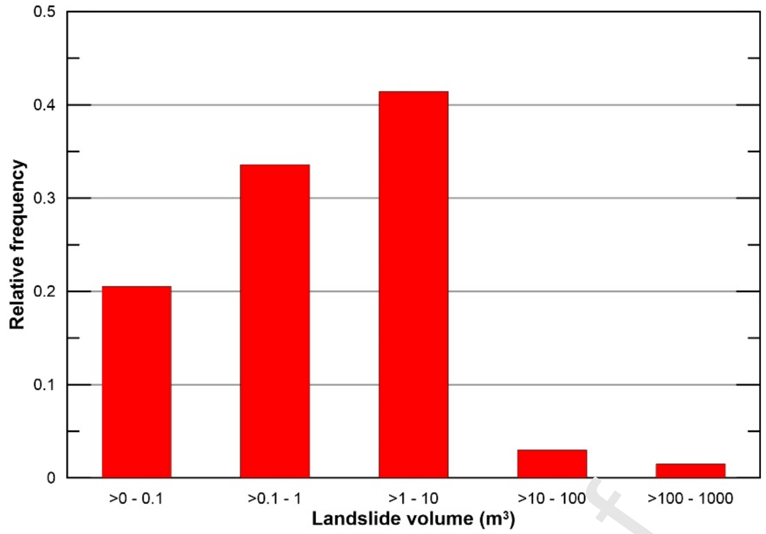

Figure 4. Estimated volume of landslides triggered by the 2011 Lorca earthquake.

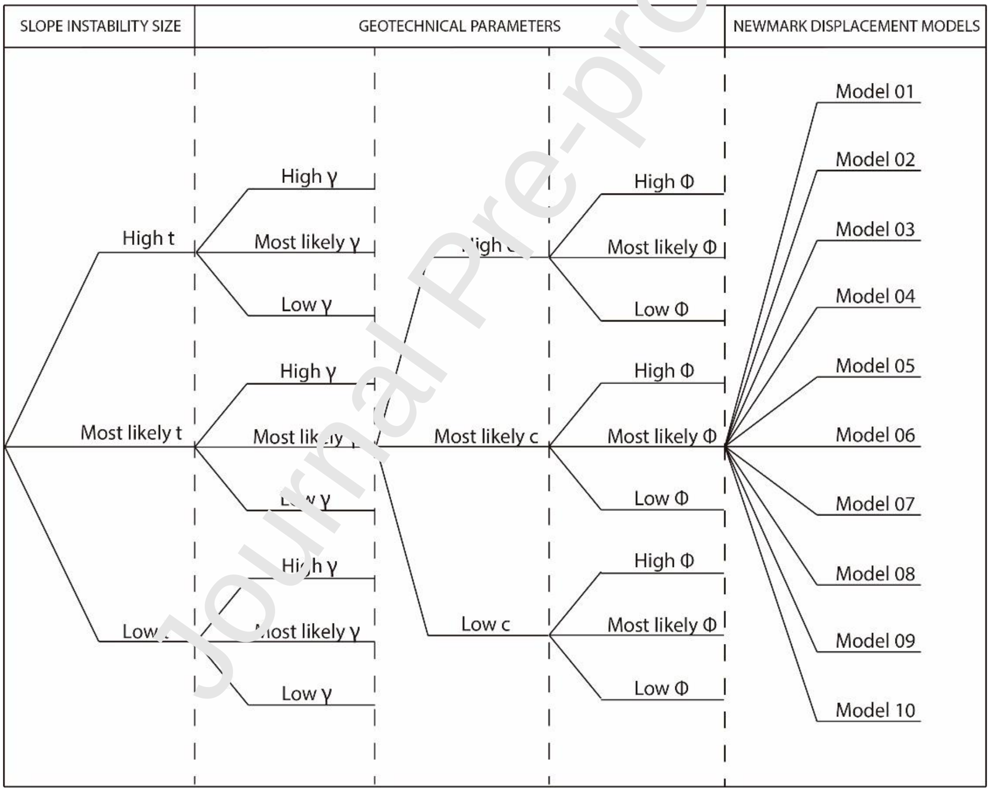

Figure 5. Example scheme of the structure of the logic tree for a probabilistic seismic landslide hazard mapping assessment.

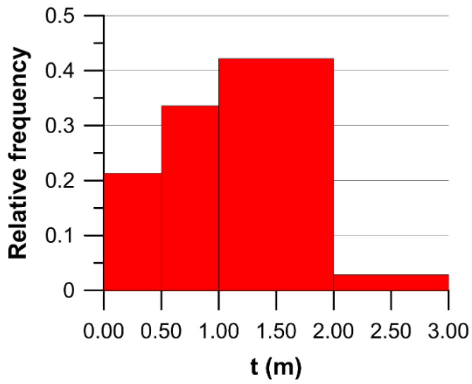

Figure 6. Estimated depth of the failure surface (t) of landslides triggered by the 2011 Lorca earthquake.

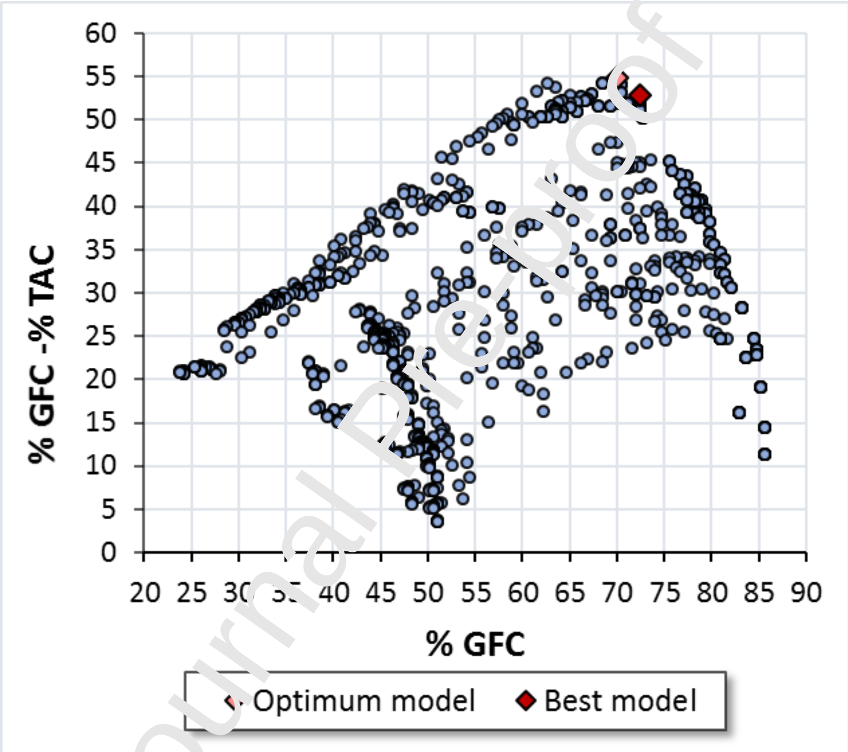

Figure 7. Parameter set efficiency referring to the models for seismic landslide hazard mapping assessment. The percentage of landslide areas correctly identified (%GFC) for each set of parameters is shown on the x-axis. Y-axis shows the efficiency difference between the percentage of landslide areas correctly identified (%GFC) and the percentage of total area identified as landslides (%TAC). The optimum model corresponds to the model with greatest value of %GFC - %TAC. The best model is the one with the greatest total weight in the logic-tree procedure.

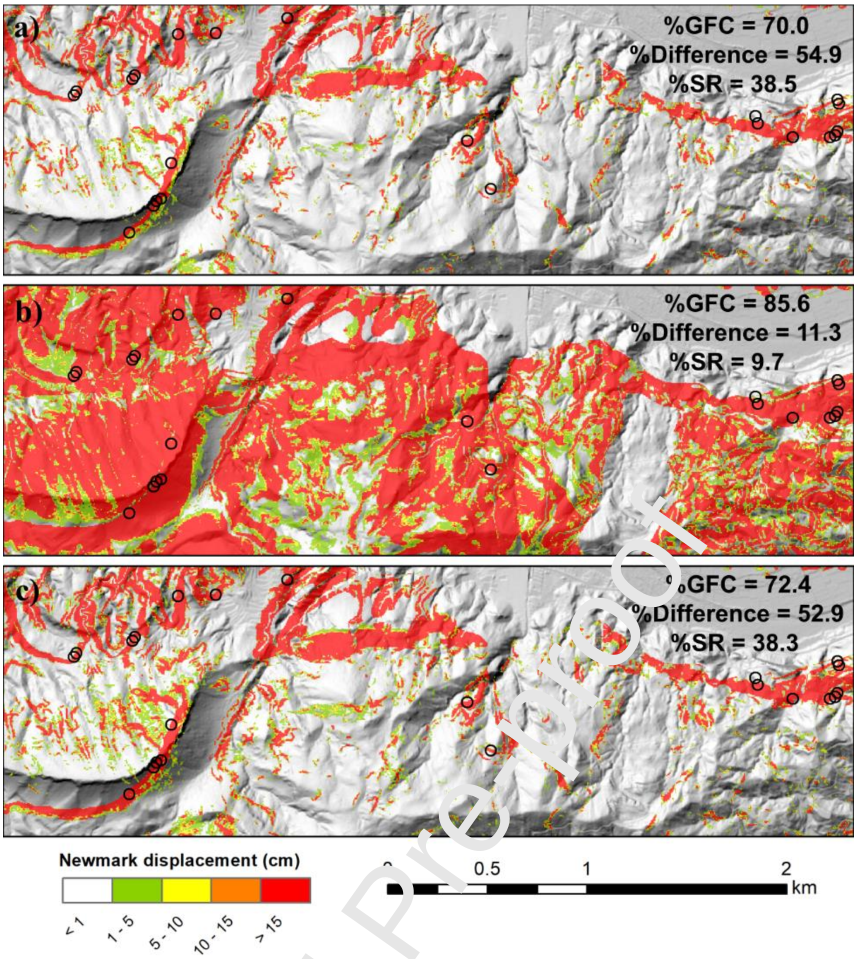

Figure 8. Excerpt of certain seismic landslide hazard maps obtained in the logic-tree procedure considering the occurrence of a moderate magnitude earthquake. **a.** Map showing the optimum model with the highest success rate (%SR). **b.** Map with the highest percentage of landslide areas correctly identified (%GFC). **c.** Map showing the best model with the highest total weight. Slope instabilities triggered by 2011 Lorca earthquake are depicted as black circles.

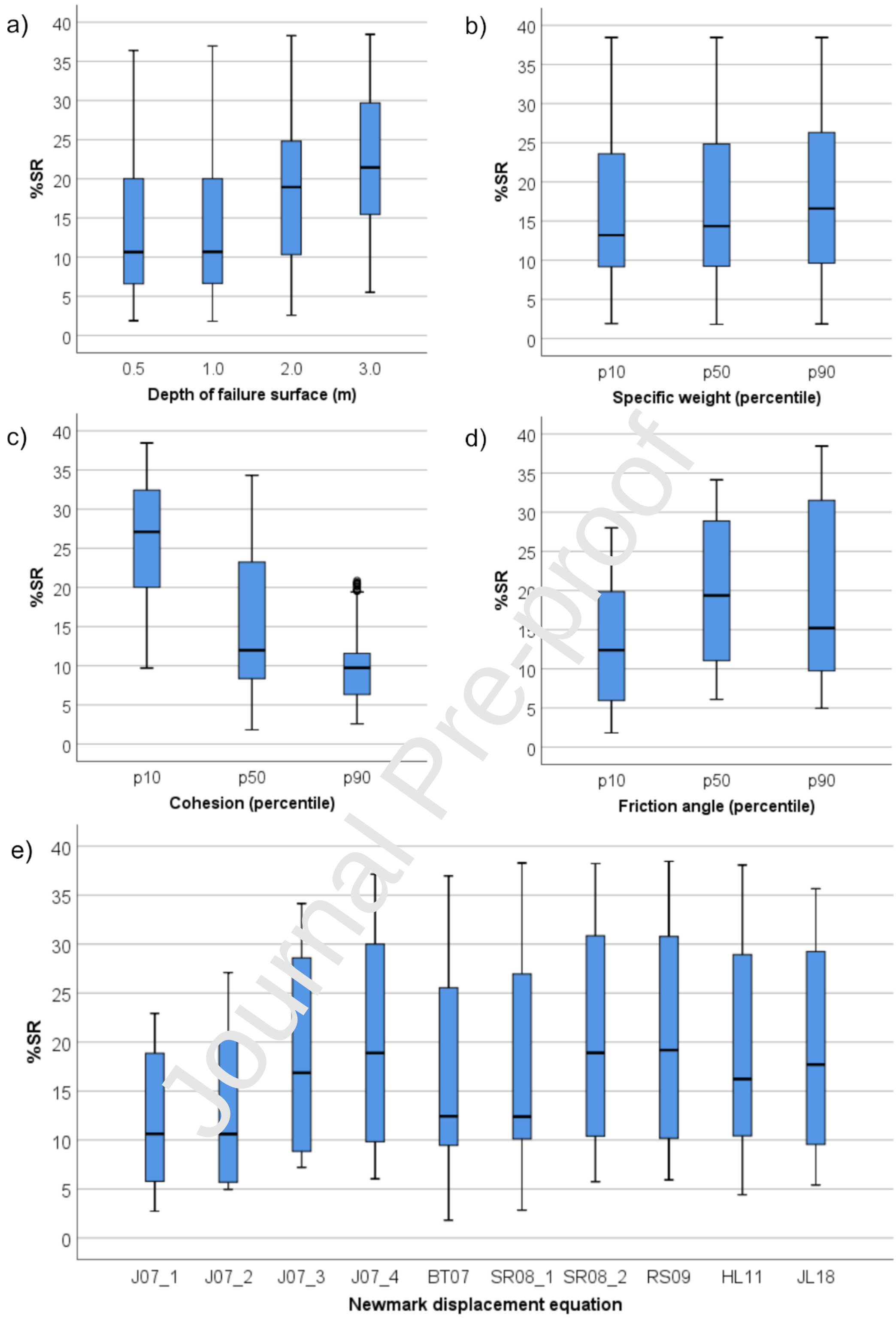

Figure 9. Distributions of success rate (%SR) considering the variability of the different variables used in the logic tree. Central lines denote the median values (50 percentile), the edges of the box mark the percentiles 25 and 75, and the tips of the whiskers represent the minimum and maximum values.

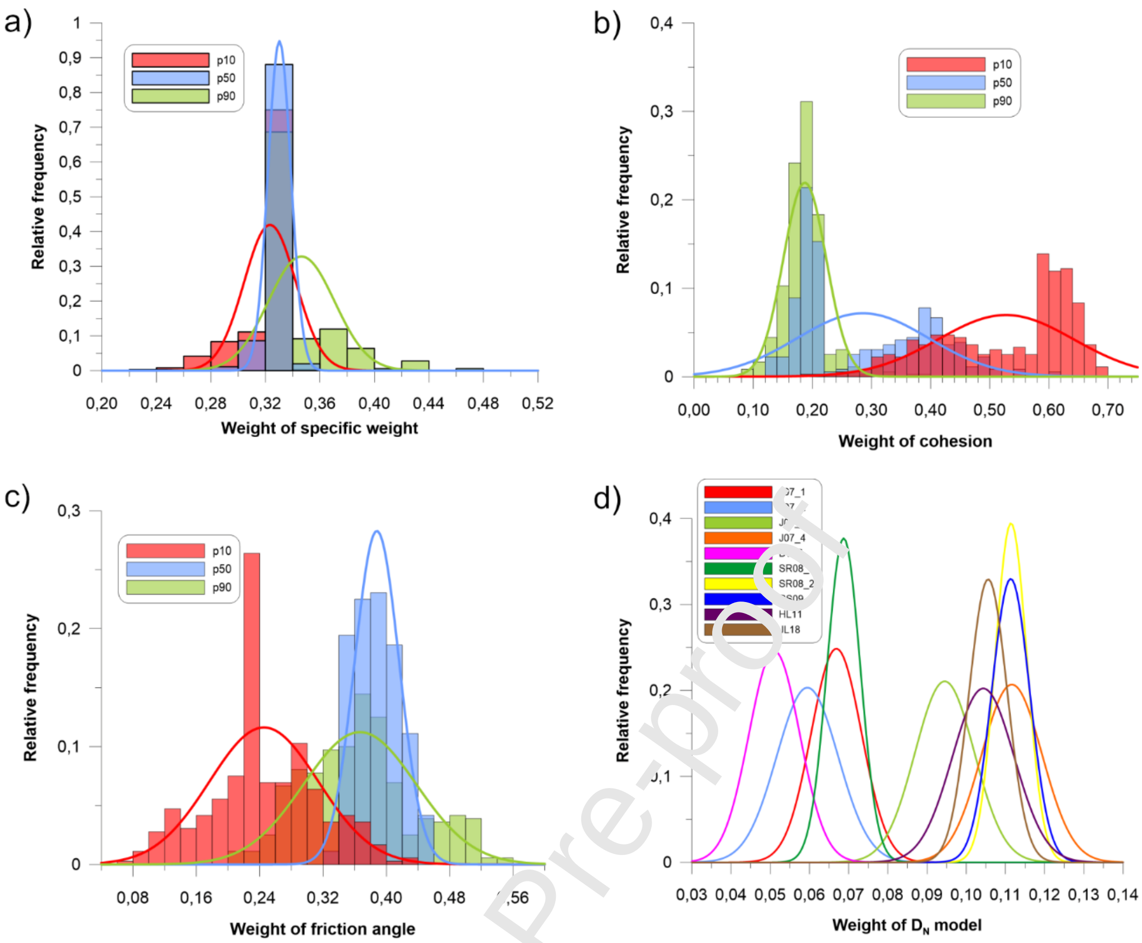

Figure 10. Distributions of weights considering the variability of the different variables used in the logic-tree procedure. Lines show the normal distribution fitting.

Table 1. Values of strength parameters for rock-type lithological groups. t: depth of the failure surface (m); ϒ: specific weight (kN/m^3); c: cohesion (kPa); Φ: friction angle (°).

		Calcareous sandstones and limestones			Conglomerates, sandstones and argillites			Phyllites and quartzites		
		ϒ	**c**	**Φ**	**ϒ**	**c**	**Φ**	**ϒ**	**c**	**Φ**
t = 0.5	Low	23.05	0.00	26	21.19	0.00	26	23.54	0.00	26
	Most likely	23.57	0.07	32	22.84	0.11	32	23.79	0.08	32
	High	24.60	0.17	39	23.89	0.30	43	24.23	0.27	42
t = 1.0	Low	23.05	0.00	26	21.19	0.00	26	23.54	0.00	26
	Most likely	23.57	0.13	31	22.84	0.20	31	23.79	0.14	32
	High	24.60	0.31	38	23.89	0.54	43	24.23	0.51	41
t = 2.0	Low	23.05	0.00	26	21.19	0.00	26	23.54	0.00	26
	Most likely	23.57	0.23	31	22.84	0.36	31	23.79	0.26	31
	High	24.60	0.57	37	23.89	0.97	41	24.23	0.91	40
t = 3.0	Low	23.05	0.00	26	21.19	0.00	26	23.54	0.00	26
	Most likely	23.57	0.33	31	22.84	0.50	30	23.79	0.37	31
	High	24.60	0.80	37	23.89	1.36	40	24.23	1.29	39

Table 2. Values of strength parameters for soil-type materials. ϒ: specific weight (kN/m^3); c: cohesion (kPa); Φ: friction angle (°).

	Marls and gypsums		
	ϒ	**c**	**Φ**
Low	16.3[illegible]	0.00	15
Most likely	17.95	15.75	21
High	20.37	30.63	28

Table 3. Newmark displacement models used in this study. Newmark displacement (D_N) is in cm, PGA and k_y are in g units (1 g = 9.81 m/s^2), I_A is in m/s, and M is the moment magnitude.

Model	Relation	Reference
J07_1	$\log D_N = 0.215 + \log\left[\left(1-\frac{k_y}{PGA}\right)^{2.341}\left(\frac{k_y}{PGA}\right)^{-1.438}\right]$	Jibson (2007)
J07_2	$\log D_N = -2.710 + \log\left[\left(1-\frac{k_y}{PGA}\right)^{2.335}\left(\frac{k_y}{PGA}\right)^{-1.478}\right] + 0.424M$	Jibson (2007)
J07_3	$\log D_N = 2.401\log I_A - 3.481\log k_y - 3.230$	Jibson (2007)
J07_4	$\log D_N = 0.561\log I_A - 3.833\log\left(\frac{k_y}{PGA}\right) - 1.474$	Jibson (2007)
BT07	$\ln D_N = -0.22 - 2.83\ln k_y - 0.333(\ln k_y)^2 + 0.566\ln k_y \ln PGA + 3.04\ln PGA - 0.244(\ln PGA)^2 + 0.278(M-7)$	Bray and Travasarou (2007)
SR08_1	$\ln D_N = 5.52 - 4.43\left(\frac{k_y}{PGA}\right) - 20.39\left(\frac{k_y}{PGA}\right)^2 + 42.61\left(\frac{k_y}{PGA}\right)^3 - 28.74\left(\frac{k_y}{PGA}\right)^4 + 0.72\ln PGA$	Saygili and Rathje (2008)
SR08_2	$\ln D_N = 2.39 - 5.24\left(\frac{k_y}{PGA}\right) - 18.78\left(\frac{k_y}{PGA}\right)^2 + 42.01\left(\frac{k_y}{PGA}\right)^3 - 29.15\left(\frac{k_y}{PGA}\right)^4 - 1.56\ln PGA + 1.38\ln I_A$	Saygili and Rathje (2008)

RS09	$\ln D_N = 4.89 - 4.85\left(\frac{k_y}{PGA}\right) - 19.64\left(\frac{k_y}{PGA}\right)^2 + 42.49\left(\frac{k_y}{PGA}\right)^3 - 29.06\left(\frac{k_y}{PGA}\right)^4 + 0.72\ln PGA + 0.89(M-6)$	Rathje and Saygili (2009)
HL11	$\log D_N = 0.847\log I_A - 10.62\,k_y + 6.587k_y\log I_A + 1.84$	Hsieh and Lee (2011)
JL18	$\log D_N = 0.465\log I_A + 12.896k_y\log I_A - 22.201k_y + 2.092$	Jia-Liang et al. (2018)

Table 4. Variation of the success rate (%SR) considering the variability of Newmark displacement regression models.

D_N model	J07_1	J07_2	J07_3	J07_4	BT07	SR08_1	SR08_2	RS09	HL11	JL18
Maximum %SR	22,92	27,09	34,14	37,14	36,97	38,28	38,23	38,45	38,07	35,66
Median %SR	10,62	10,61	16,86	18,88	12,43	12,39	[illegible]	19,18	16,23	17,70
Mean %SR	11,81	13,51	18,94	18,96	16,95	17,62	[illegible]	18,97	18,20	18,06

Table 5. Weights obtained for different Newmark displacement regression models in the logic-tree procedure.

D_N model	J07_1	J07_2	J07_3	J07_4	BT07	SR08_1	SR08_2	RS09	HL11	JL18
Mean Weight	0,0669	0,0803	0,1133	0,1116	0,0946	0,1000	0,1114	0,1113	0,1050	0,1056
Median Weight	0,0673	0,0789	0,1149	0,1119	0,0928	0,0990	0,1115	0,1110	0,1058	0,1069

Highlights

- A new method to obtain unbiased logic-tree weights in a probabilistic earthquake-induced landslide hazard analysis.
- Influence of different variables and uncertainties in the resulting earthquake-induced landslide hazard maps.
- An improvement of the well-known Newmark method is proposed.
- The obtained weights can be applied to seismically-induced landslide hazard maps assessments in low to moderate magnitude seismic areas.